Supplementary Information

Lotus pollen extract regulated calcium carbonate hollow nanospheres as efficient mitochondria-targeted drug carrier

Jie Zhang,[a] Yi Chang,[a] Han Li,[b] Weike Shi,[b] Zhihao Chen,[a] Lina Ding,[b] Xinhe Liu,[b] Xiaoming Ma*[b] and Yuming Guo*[a]*

[a] *Key Laboratory of Green Chemical Media and Reactions, Ministry of Education, Henan Normal University, Xinxiang, Henan 453007, China.*

[b]*Collaborative Innovation Center of Henan Province for Green Manufacturing of Fine Chemicals, School of Chemistry and Chemical Engineering, Henan Normal University, Xinxiang, Henan 453007, China.*

Experimental Procedures

Characterization

The field emission-scanning electron microscopy (FE-SEM, SU8010, Hitachi) was used to characterize the morphologies and sizes of the as-prepared products. The internal structure of the product was investigated using the JEOL JEM-2100 transmission electron microscope (TEM) equipped with a selected-area electron diffraction (SAED). The composition and crystalline property of the products were characterized by the powder X-ray diffraction (XRD) using a Bruker D8 & Advance X-ray powder diffractometer with graphite monochromatized Cu Kα radiation (λ = 0.15406 nm, 2θ range: 20-70°). The Fourier transform infrared (FT-IR) spectra were determined by using the Bio-Rad FTS-40 FT-IR spectrometer (the wavenumber range: 4000–400 cm-1). The thermogravimetry-differential scanning calorimetry (TG-DSC) experiments were carried out on the NETZSCH STA 449C with a linear heating rate of 10 °C/min in the temperature range of 25-1000 °C under air atmosphere. The common used log normal function from 100 nanospheres in a randomly area was chosen to evaluate the size distribution of the samples. The component analysis of biomolecules in the samples is entrusted to Qingdao Sci-tech Innovation Quality Testing Co., Ltd. China.

Cell culture

In the present study, V79-4 Chinese hamster lung cells and HeLa human cervical carcinoma cells were selected as the model normal and cancer cells, respectively. The cells were cultivated in Eagle's minimum essential medium (EMEM) supplemented with heat-inactivated FBS (10%), Penicillin (100 units mL^{-1}), Streptomycin (100 μg mL^{-1}), amphotericin B (fungizone, 0.25 μg mL^{-1}) and sodium bicarbonate (2.2 μg mL^{-1}) in a humidified incubator with 5% CO_2 at 37 ℃

Anti-proliferative effects evaluation

HeLa or V79-4 single-cell suspensions (100 μL) with initial cell density of 2.5×10^4 cells mL^{-1} were pre-seeded separately in each well of 96-well flat bottom culture microplates for 24 h. Subsequently, free DOX and $CaCO_3$/SFLP/DOX suspension in EMEM medium were added into the wells and co-incubated for 120 h. The final concentrations of DOX were 0.0977, 0.1953, 0.3906, 0.7813, 1.5625, 3.125, and 6.25 μg mL^{-1}, respectively. Incubation of cells with EMEM medium rather than samples was prepared as the control. The anti-proliferative effects of the free DOX and $CaCO_3$/SFLP/DOX

on V79-4 and HeLa cells were measured by MTT colorimetric assay. Briefly, after 120 h treatment, freshly prepared MTT solution (100 μL, 5 mg mL^{-1} in PBS) was added to each well and incubated at 37 °C for 5 h. After carefully discard the supernatant in each well, the dark blue crystals were dissolved completely by 150 μL of DMSO and the absorbance of the solution in each well at 570 nm was quantified by a microplate reader. The cell proliferation activity was expressed by the absorbance while the cytotoxic effects of the free DOX and $CaCO_3$/SFLP/DOX were calculated by Equation 1. The data were reported as mean ± SD based on triplicate measurements.

$$\text{Percentage of inhibition (\%)} = \left(1 - \frac{\text{O.D.}_{570\text{nm}} \text{ of treatment group}}{\text{O.D.}_{570\text{nm}} \text{ of control group}}\right) \times 100 \quad (1)$$

Determination of intracellular [Ca^{2+}]

To determine [Ca^{2+}], $CaCO_3$/SFLP/DOX was co-incubated with V79-4 or HeLa cells for 72 h. Subsequently, the culture flasks were gently rinsed with ultrapure water to remove any possible solid samples completely. Then the cells were collected, digested with concentrated nitric acid, and analyzed using inductively coupled plasma-mass spectrometer (ICP-MS, ELAN DRC-e, Perkin–Elmer Sciex) to determine [Ca^{2+}]. For comparison, [Ca^{2+}] in the control cells were also determined.

CLSM evaluation for the specific uptake of $CaCO_3$/SFLP/DOX by cancer cells

Cells with an initial density of 2 × 10^5 cells mL^{-1} were seeded in confocal dish with cover glass bottom for 24 h. Then, the cells were treated by $CaCO_3$/SFLP/DOX for 12 h and stained with tetracycline hydrochloride. After washed with PBS for three times, the cells were observed by Carl Zeiss Cell Observer (Jena, Germany). The treatment with culture medium was prepared as control. Calcium staining by tetracycline hydrochloride: scan range = 550 ± 15 nm excited at 405 nm (green channel). DOX autofluorescence: excitation wavelength = 488 nm, scan range = 590 ± 15 nm (red channel).

Apoptosis and necrosis evaluation

The percentages of apoptotic and necrotic cells were determined by flow cytometric analysis. HeLa cancer cells and V79-4 normal cells with an initial density of 1 × 10^6 cells mL^{-1} were seeded for 24 h. Then the cells were treated by DOX or $CaCO_3$/SFLP/DOX for 48 h. The treatment of cells with culture medium was prepared as control. After treatment, the cells were collected. The

quantification of apoptosis and necrosis was determined by flow cytometric analysis with an Annexin V-FITC/PI double staining assay. Briefly, the collected cells were harvested with an EDTA-free trypsin solution and treated with Annexin V-FITC and PI for at least 10 min at room temperature under dark. Then Annexin V binding buffer was added. The solution was filtered and immediately analyzed using Cytomics FC500 flow cytometer (Beckman Coulter, USA).

Characterization of $CaCO_3$/SFLP HNSs

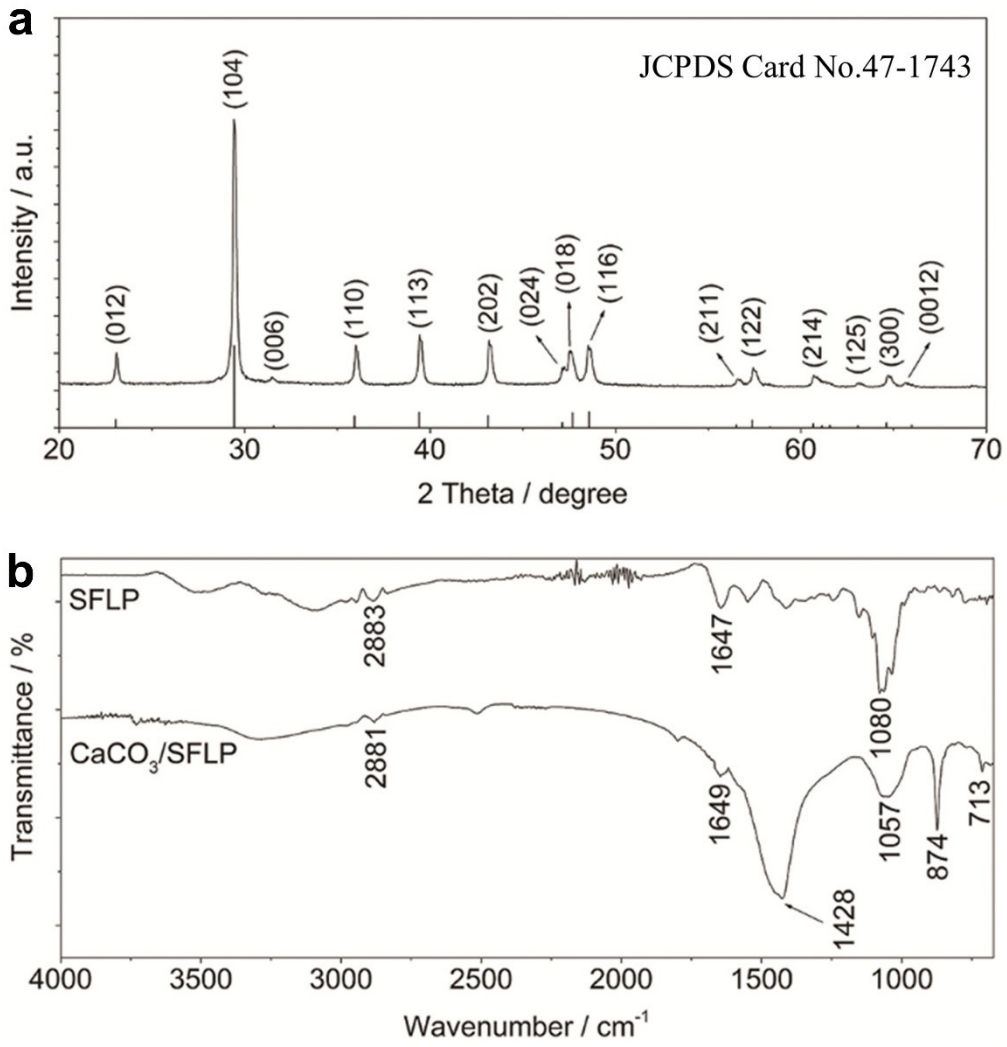

Fig. S1. (a) XRD pattern of $CaCO_3$/SFLP HNSs and (b) FT-IR spectra of SFLP and $CaCO_3$/SFLP HNSs.

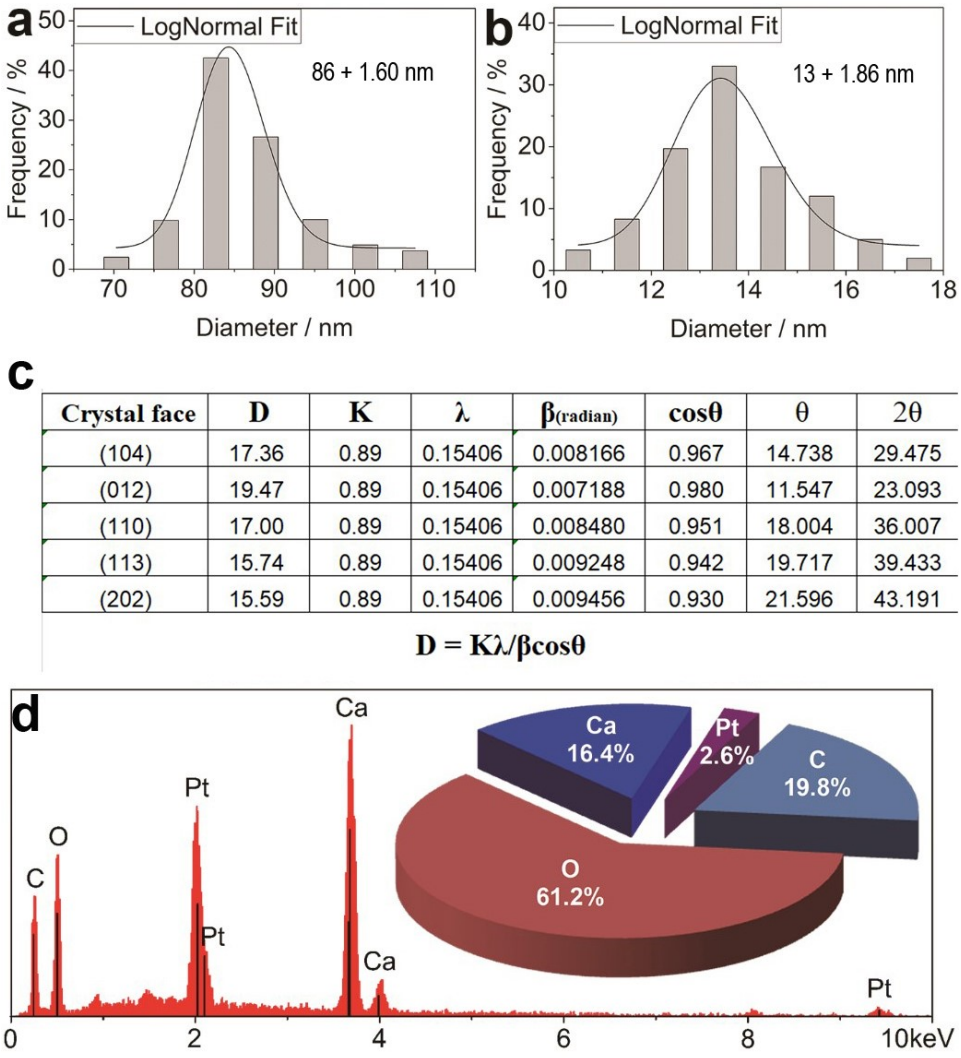

c

Crystal face	D	K	λ	β(radian)	cosθ	θ	2θ
(104)	17.36	0.89	0.15406	0.008166	0.967	14.738	29.475
(012)	19.47	0.89	0.15406	0.007188	0.980	11.547	23.093
(110)	17.00	0.89	0.15406	0.008480	0.951	18.004	36.007
(113)	15.74	0.89	0.15406	0.009248	0.942	19.717	39.433
(202)	15.59	0.89	0.15406	0.009456	0.930	21.596	43.191

$$D = K\lambda/\beta\cos\theta$$

Fig. S2. Size distribution analysis of (a) $CaCO_3$/SFLP HNSs and (b) the nanoclusters in $CaCO_3$/SFLP HNSs. (c) The calculated results of nanoparticle size based on Scherrer equation. (d) EDS spectrum of $CaCO_3$/SFLP HNSs. Inset: Atomic percentages of different elements in $CaCO_3$/SFLP HNSs.

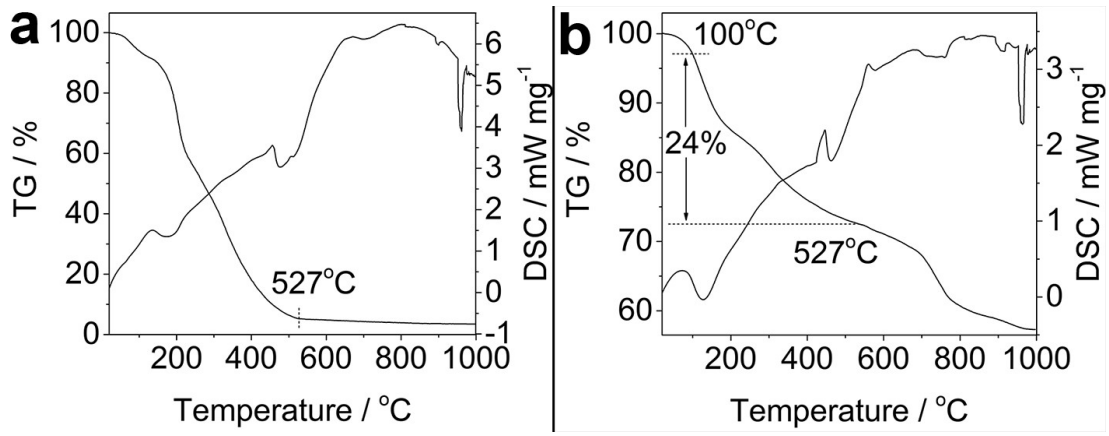

Fig. S3. TG-DSC curves of (a) SFLP and (b) $CaCO_3$/SFLP HNSs.

The formation process of $CaCO_3$/SFLP HNSs at different time stage

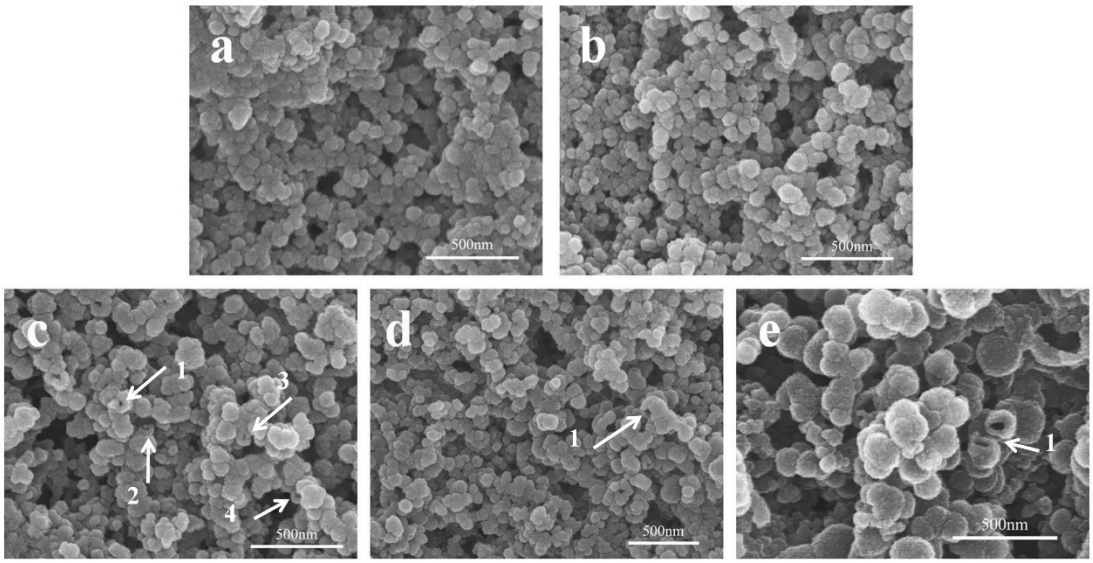

Fig. S4. The formation process of $CaCO_3$/SFLP HNSs under the regulation of SFLP at different stage. (a) 0 min; (b) 30 min; (c) 1 h; (d) 1.5 h; (2) 2h.

The formation mechanism of $CaCO_3$/SFLP HNSs

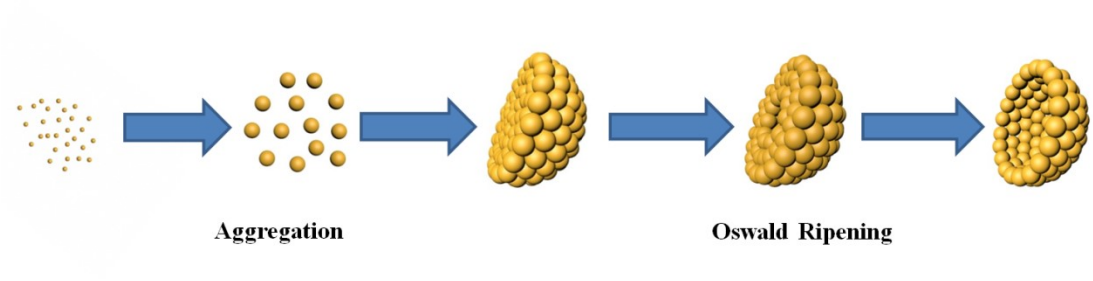

Fig. S5. The speculated mechanism in the formation of $CaCO_3$/SFLP HNSs.

CLSM observation of DOX loading onto $CaCO_3$/SFLP HNSs

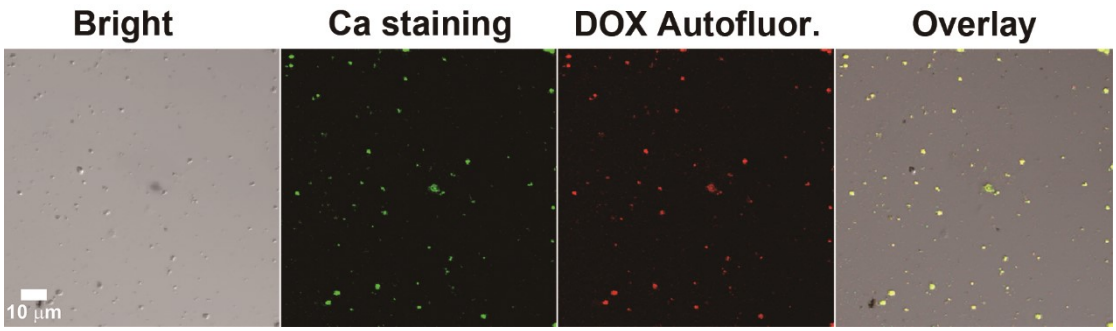

Fig. S6. CLSM images of $CaCO_3$/SFLP/DOX. Ca staining: excitation wavelength = 405 nm, scan range = 550 ± 15 nm (green channel). DOX autofluorescence: excitation wavelength = 488 nm, scan range = 590 ± 15 nm (red channel).

FE-SEM observation of $CaCO_3$/SFLP/DOX after incubated in release buffer

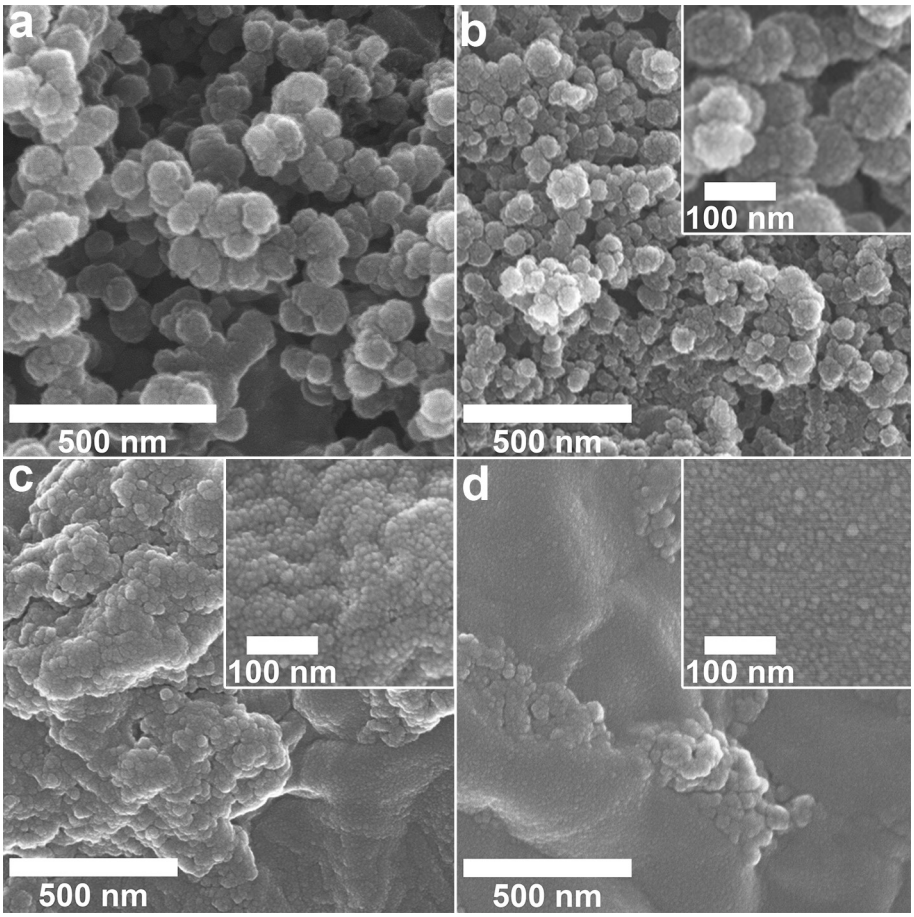

Fig. S7. FE-SEM images of (a) raw $CaCO_3$/SFLP/DOX and $CaCO_3$/SFLP/DOX incubated in release buffer with different pH values. (b) pH = 7.4; (c) pH = 6.0; (d) pH = 5.0.

***In vitro* cytotoxicities of $CaCO_3$ and $CaCO_3$/SFLP**

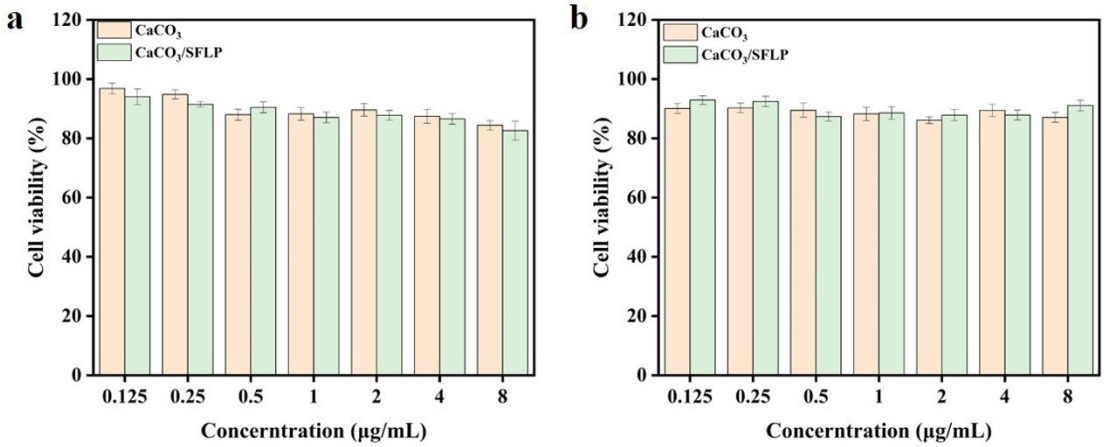

Fig. S8. *In vitro* cytotoxicities of $CaCO_3$ and $CaCO_3$/SFLP on V79-4 cells (a) and HeLa cells (b) after incubation for 5 days.

Uptake of $CaCO_3$/SFLP/DOX by normal cells

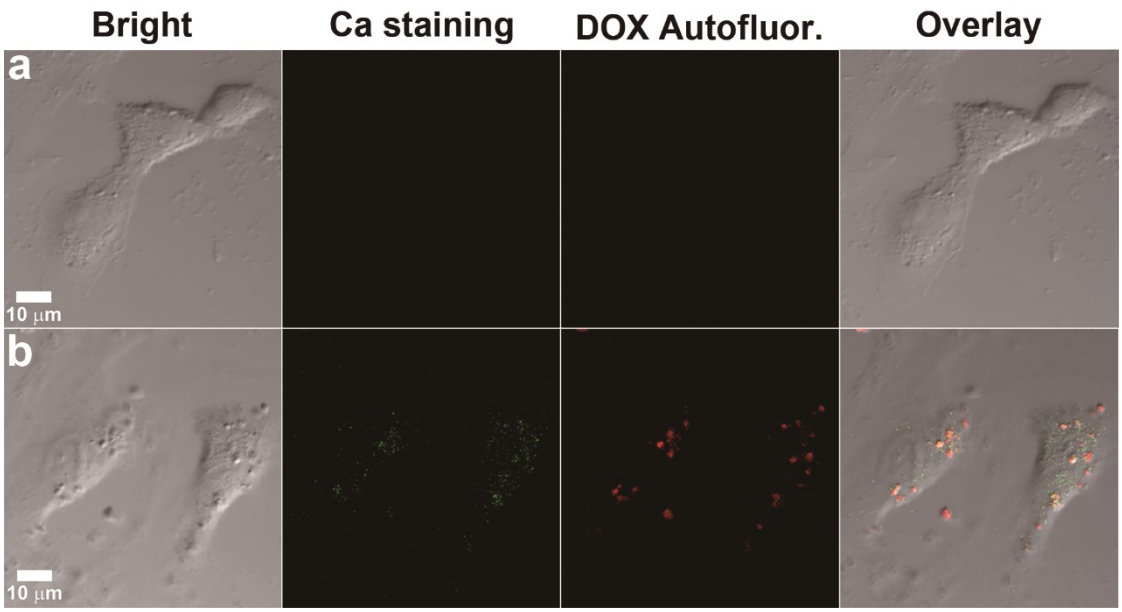

Fig. S9. CLSM images of (a) control V79-4 cells and (b) V79-4 cells treated by $CaCO_3$/SFLP/DOX for 12 h. Ca staining: excitation wavelength = 405 nm, scan range = 550 ± 15 nm (green channel). DOX autofluor.: excitation wavelength = 488 nm, scan range = 590 ± 15 nm (red channel).

Distribution of $CaCO_3$/SFLP/DOX in subcellular organelles of cancer cells

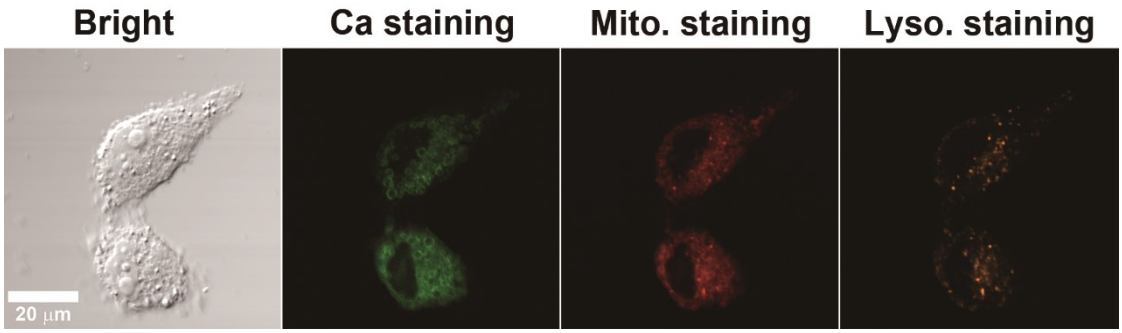

Fig. S10. CLSM images of HeLa cells treated by $CaCO_3$/SFLP/DOX for 0.5 h. Ca staining: excitation wavelength = 405 nm, scan range = 550 ± 15 nm (green channel). Mitochondria staining: excitation wavelength = 635 nm, scan range = 660 ± 15 nm (red channel). Lysosome staining: excitation wavelength = 559 nm, scan range = 600 ± 15 nm (orange channel).

Component analysis of $CaCO_3$/SFLP

Table S1 Amino acids contained in $CaCO_3$/SFLP.

	Amino acid names	Content (g / 100 g)
1	Arginine	0.013
2	Aspartate	0.003
3	Glutamate	0.0018
4	Serine	0.0069
5	Cystine	0.0069

Experimental study of subcellular colocalization analysis

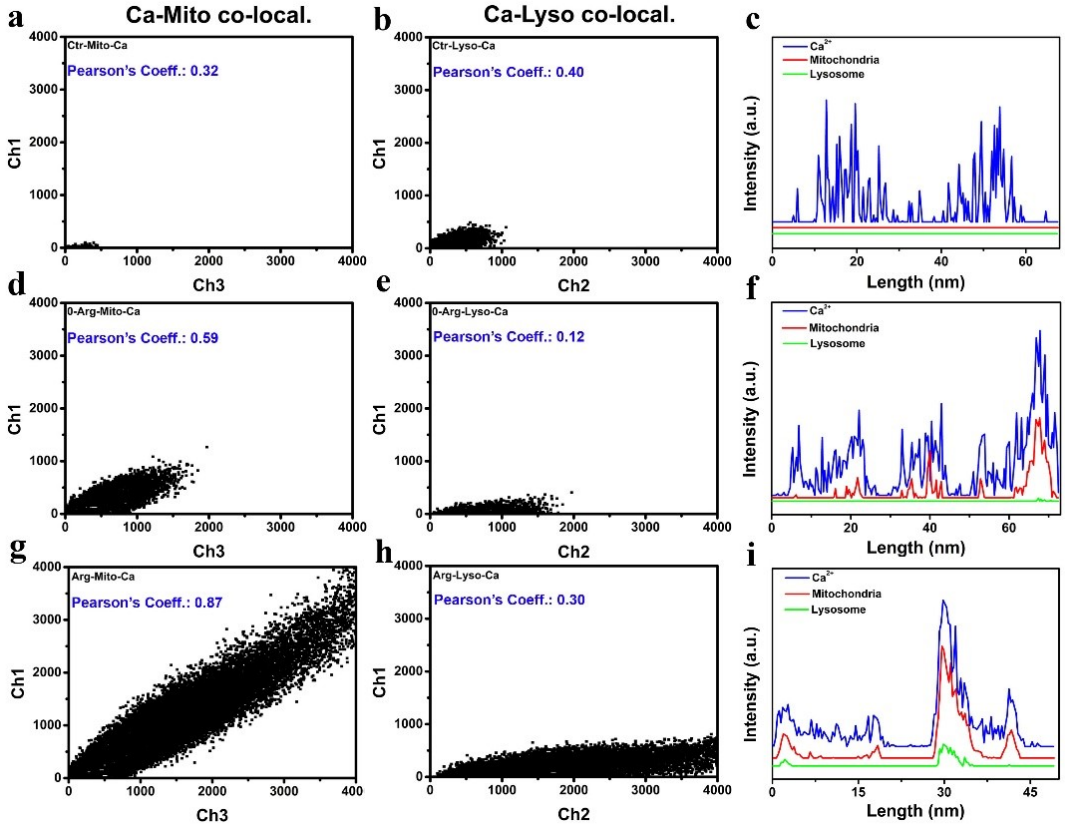

Fig. S11. Intensity correlation plots of calcium in mitochondria and lysosome of HeLa cells, respectively. (a-c) the control group; (d-f) the group of $CaCO_3$ without Arginine; (g-i) the group of $CaCO_3$ with Arginine.

FE-SEM observation of $CaCO_3$ under the regulation of Arginine

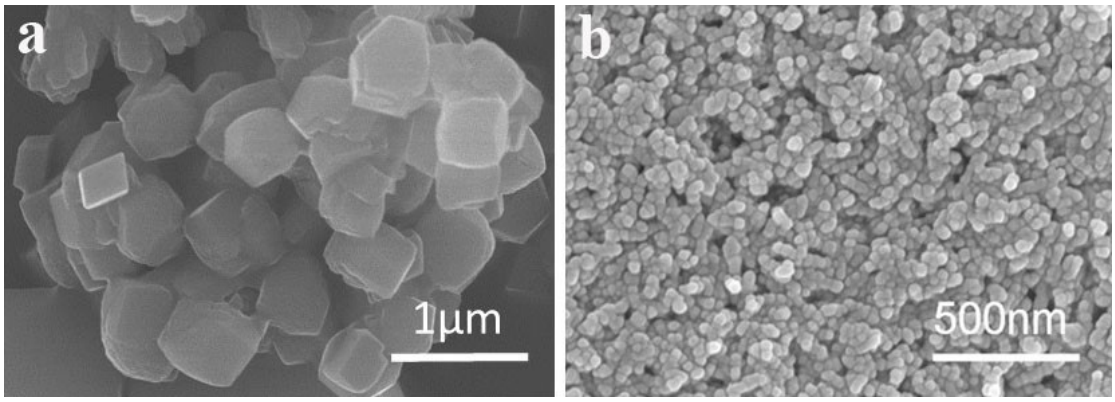

Fig. S12. FE-SEM images of the groups of $CaCO_3$ synthesized (a) without the regulation of Arginine and (b) with the regulation of Arginine.